



HAL
open science

The relative influence of the topography and chemistry of TiAl6V4 surfaces on osteoblastic cell behaviour

Karine Anselme, P. Linez, Maxence Bigerelle, D. Le Maguer, A. Le Maguer, P. Hardouin, H.F. Hildebrand, Alain Iost, J.M. Leroy

► To cite this version:

Karine Anselme, P. Linez, Maxence Bigerelle, D. Le Maguer, A. Le Maguer, et al.. The relative influence of the topography and chemistry of TiAl6V4 surfaces on osteoblastic cell behaviour. *Biomaterials*, 2000, 21 (15), pp.1567-1577. 10.1016/S0142-9612(00)00042-9 . hal-02566284

HAL Id: hal-02566284

<https://hal.science/hal-02566284>

Submitted on 17 Apr 2024

HAL is a multi-disciplinary open access archive for the deposit and dissemination of scientific research documents, whether they are published or not. The documents may come from teaching and research institutions in France or abroad, or from public or private research centers.

L'archive ouverte pluridisciplinaire **HAL**, est destinée au dépôt et à la diffusion de documents scientifiques de niveau recherche, publiés ou non, émanant des établissements d'enseignement et de recherche français ou étrangers, des laboratoires publics ou privés.

The relative influence of the topography and chemistry of TiAl6V4 surfaces on osteoblastic cell behaviour

K. Anselme^{a,*}, P. Linez^b, M. Bigerelle^c, D. Le Maguer^d, A. Le Maguer^d, P. Hardouin^a, H.F. Hildebrand^b, A. Iost^c, J.M. Leroy^d

^aIRMS, Institut Calot, rue du Dr Calot, 62608 Berck sur mer, France

^bGRB, Faculté de Médecine, Place de Verdun, 59045 Lille, France

^cENSAM, 8 bd Louis XIV, 59046 Lille, France

^dENSCL, BP 108, 59652 Villeneuve d'Ascq, France

Abstract

Proliferation and adhesion of mouse (MC3T3-E1) osteoblastic cells and primary human osteoblastic cells were carried out on Ti6Al4V titanium alloy samples with varied surface roughnesses. Mechanically or manually polished surfaces were prepared to produce respectively non-oriented or oriented residual polishing grooves. Sand-blasted surfaces were prepared using 500 µm or 3 mm alumina particles. Surface roughness parameters showed a negative correlation in comparison to proliferation and adhesion parameters. X-ray microprobe chemical surface microanalysis showed complete disturbance of the surface element composition of the Ti6Al4V alloy following sand-blasting treatment. An AlO_x-enriched layer was observed on sample surfaces. This may lead to the suspicion that the concomitant effect of surface roughness amplitude and AlO_x surface concentration has an effect on osteoblastic cell proliferation and adhesion. These findings show the significance of chemical surface analysis after any surface treatment of titanium-based implants before any biological use. © 2000 Elsevier Science Ltd. All rights reserved.

Keywords: Surface chemistry; Surface topography; Titanium alloy; Cell proliferation; Cell adhesion; Osteoblast

1. Introduction

Titanium and titanium alloys are largely used as implant materials because of their high in vitro [1–4] and in vivo biocompatibility [5–10]. Nevertheless, some concern remains as to the effects of vanadium and aluminium which are known to be cytotoxic [11–16]. To improve the bone integration of titanium-based implants, surface treatments such as surface machining, acid etching, electropolishing, anodic oxidation, sand blasting or plasma-spraying may be undertaken [5,9,17–22]. However, in the field of metallurgy, these surface treatments are known to induce chemical modifications of the implant, associated with the modifications of surface topography [22]. In the field of biomaterials, many studies

have independently considered the surface topography and surface chemistry effects on in vitro and in vivo biocompatibility with bone but few have considered their simultaneous biological effects [5–10,18–21]. In this study we attempted to perform a concomitant analysis of the roughness and chemistry of polished and sand-blasted titanium alloy surfaces. The in vitro cytocompatibility of these surfaces, evaluated by use of a mouse (MC3T3-E1) osteoblastic cell line and primary human osteoblastic cells, is discussed in relation to the topography and chemistry of tested surfaces.

2. Materials and methods

2.1. Materials

Discs of a Ti6Al4V-ELI alloy (medical quality), 14 mm in diameter and 2 mm in height, were processed by

*Corresponding author. Tel.: + 33-321-892029; fax: + 33-321-892070.

E-mail address: kanselme@hopale.com (K. Anselme).

sand-blasting (500 μm or 3 mm alumina particles) or by polishing with P4000, P1200, P80 silicon carbide paper or diamond paste (0.25 μm particles) (mirror-polish). Polishing with P4000, P1200 or P80 silicon carbide paper was performed mechanically or manually to induce a parallel orientation of residual grooves. Metallic substrates were rinsed twice in absolute alcohol and once in demineralized water in ultrasound, before sterilization by heat for testing with human osteoblasts or by steam for testing using MC3T3-E1 osteoblasts. Some additional sand-blasted samples were prepared using silicon carbide particles as controls for WDS analysis.

2.2. Cell culture

A mouse osteoblast-like cell line (MC3T3-E1) was cultured in a 50/50 α -minimal essential medium (α MEM)/Dulbecco's modified essential medium (DMEM) (Gibco BRL, France) containing 10% of a 50/50 mixture of fetal calf serum and newborn calf serum, 100 units/ml of penicillin, 100 $\mu\text{g}/\text{ml}$ of streptomycin and 100 units/l of mycostatin.

Human osteoblasts were obtained from trabecular bone taken from the iliac crest of a nine-year-old patient. Cells were initially cultured in DMEM (Eurobio, France) containing 10% fetal bovine serum, 100 units/ml of penicillin, and 100 $\mu\text{g}/\text{ml}$ of streptomycin, until confluence and were then preserved in liquid nitrogen in complete DMEM + 10% dimethylsulfoxide (DMSO) (Sigma, L'Isle d'Abeau, France) for several months. The cells were then thawed and cultured in 75 cm^2 flasks. At confluence, the cells were harvested using trypsin-EDTA and inoculated onto samples in 24-well plates for proliferation and adhesion tests. Medium was changed twice a week.

2.3. Cell morphology

The cell layers were fixed, dehydrated in graduated alcohol, critical-point dried (Emscope CPD 750, Elexience, France), sputter-coated (Emscope SC 500, Elexience, France) and examined using a Hitachi S520 scanning electron microscope (Elexience, France).

2.4. Adhesion tests

Twenty-five samples of each surface were inoculated with 2×10^4 human osteoblasts/sample. Five mechanically polished samples were analysed after each incubation period: 24 h, 3, 7, 14 and 21 d. To eliminate nonviable cells, samples were rinsed three times by PBS. Then, the viable cells were enzymatically detached from the samples by a diluted trypsin-EDTA (0.025% v/v) treatment. Cells detached after 5, 10, 20, 30 and 60 min

were counted with a Coulter Z1 (Beckman-Coulter, Roissy, France). The curve of the percentage of released cells versus trypsinisation time was established. The area included between the curve and the X-axis was evaluated by integration. The areas obtained were designated as a detachment index which was inversely proportional to the cell adhesion on biomaterial [23].

2.5. Proliferation tests

2.5.1. MC3T3-E1 mouse osteoblastic cells

MC3T3-E1 cells were inoculated at 5000 cells/ cm^2 onto five manually polished samples of each roughness type in 24-well tissue culture polystyrene plates. Three additional wells served as controls. After three days of culture, the cells were enzymatically detached by a trypsin-EDTA (0.25% v/v) treatment and counted with a Coulter Z1 (Beckman-Coulter, Roissy, France). Experiments were reproduced five-times. The proliferation rate was expressed as the percentage of cells/ cm^2 on Ti6Al4V surfaces compared with polystyrene control surfaces.

2.5.2. Primary human osteoblastic cells

The proliferation curves of human osteoblasts were established from the total detached cell count obtained during the cell adhesion test after each incubation period. Areas included between these curves and the X-axis were evaluated by integration. The areas obtained were designated as a proliferation index.

2.6. Roughness measurement

Six three-dimensional surfaces were measured using a laser confocal scanning microscope (Lasertek, Elexience, France) on five samples for the six types of roughnesses. The three-dimensional surfaces were digitized into 1024×256 points that give a scanning surface of $60 \mu\text{m}^2$. Surfaces were straightened up using the least-squares method and no filtering was used to analyse surface topographies. Then usual roughness parameters were computed: R_a (average roughness), Z_{max} (maximal amplitude of roughness), Z_{min} (minimal amplitude of roughness), $R_t = Z_{\text{max}} - Z_{\text{min}}$ (range amplitude of roughness).

2.7. Chemical surface characterization by electron microprobe microanalysis (EMMA)

2.7.1. Materials

One sample of each roughness type was prepared for a surface analysis. Additional qualitative and quantitative section analysis were carried out on an alumina and

silicon carbide sand-blasted specimen. Before surface analysis, only a vacuum deposit of a thin (~ 20 nm) carbon film was applied to each sample in order to produce a conductive surface.

For the section studies, the mode of preparation consisted of embedding the samples in a cold-setting resin (Araldite®). After the polymerization of this resin, specimens were mechanically polished (final polishing with a 1 μm diamond paste) and then coated with carbon film.

2.7.2. EMMA measurements

The chemical surface composition and depth profiles of the elements were carried out by an automatic CAMEBAX-Micro microprobe (Cameca, France). Accelerating voltage was chosen in order to limit the volumes affected by the X-ray emission of the different elements.

Table 1
Statistics of roughness measures on samples^a

	R_a (μm)	R_t (μm)	Z_{max} (μm)	Z_{min} (μm)
Mirror-polished	0.16	1.46	0.73	-0.73
P4000	0.3	4.69	1.53	-3.16
P1200	0.43	5.69	2.21	-3.48
P80	0.61	5.29	2.27	-3.02
S500 μm	2.19	16.08	10.63	-5.46
S3 mm	3.4	24.76	16.25	-8.42

^aData are means of six measures. R_a is the average roughness, Z_{max} is the maximal amplitude of roughness, Z_{min} is the minimal amplitude of roughness and R_t is the range amplitude of roughness ($Z_{\text{max}} - Z_{\text{min}}$).

With the beam voltage of 10 kV the K_α characteristic lines of O, Al, Ti and the K_β characteristic line of V were analysed by the wave dispersion scanning technique (WDS) on the respective dispersive crystals: PC2®

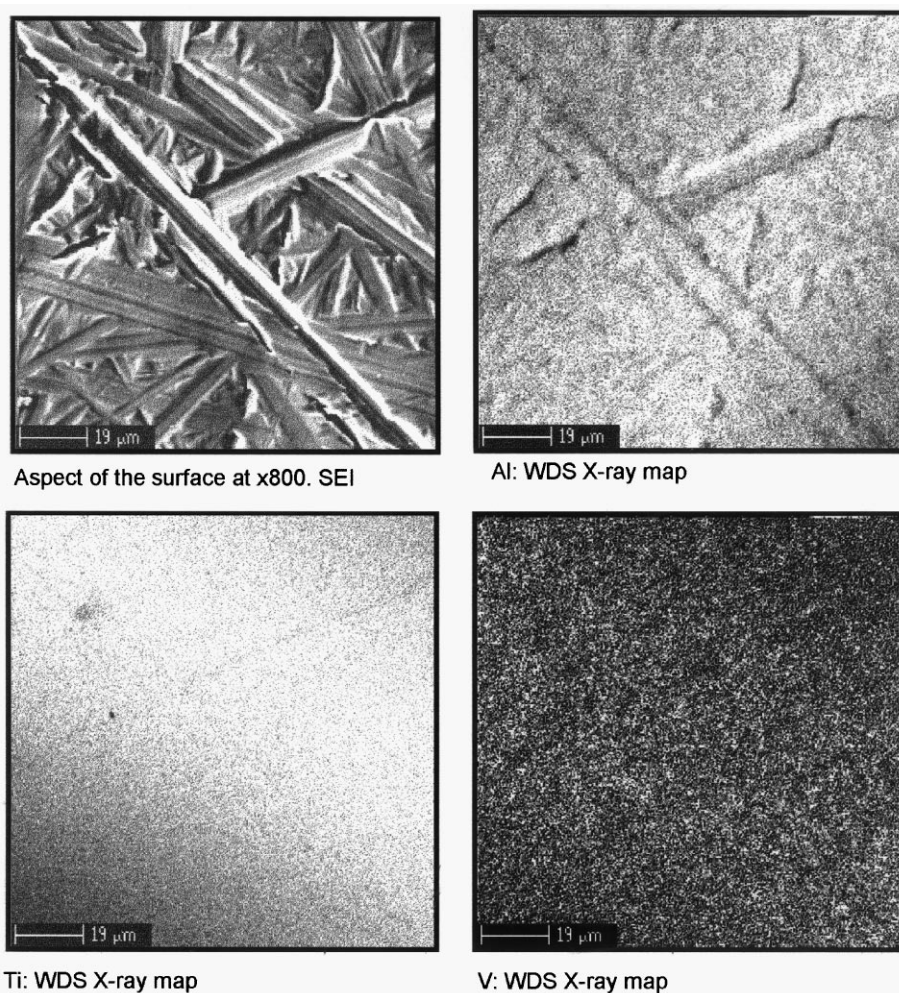
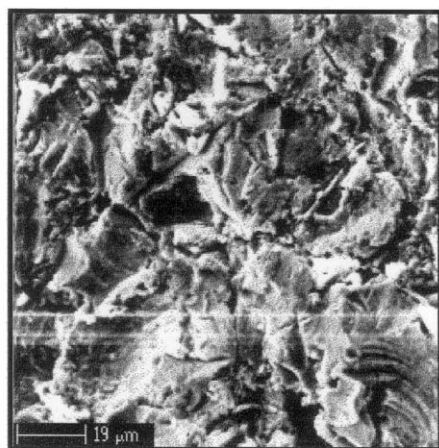
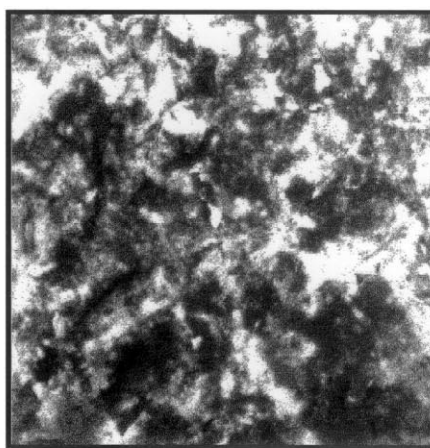


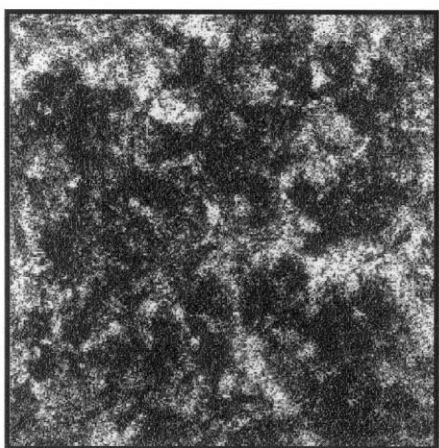
Fig. 1. WDS analysis of P80 mechanically polished surface. The topographical distribution of Al, Ti, and V was not disturbed (magnification: $\times 800$).



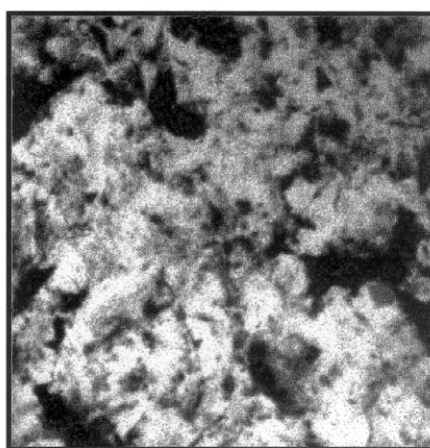
Aspect of the surface at x800. SEI



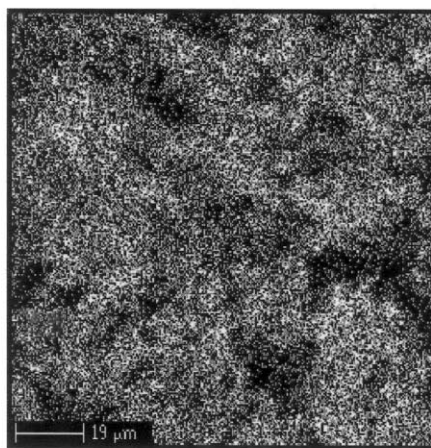
Al: WDS X-ray map



O: WDS X-ray map



Ti: WDS X-ray map



V: WDS X-ray map

Fig. 2. WDS analysis of 500 μm alumina particles sand-blasted surface. The topographical distribution of Al, Ti, and V was completely disturbed (magnification: $\times 800$).

(Cameca, France), TAP (thallium acid phthalate) and PET (pentaerythritol) (Ti and V). The selected standards were Al_2O_3 , TiMnO_3 and vanadinite (V standard). The probe intensity was automatically regulated at 40 nA.

Counting time on samples and standard was 30 s. Weight concentrations were calculated according to the well-known ZAF method (atomic number, absorption and fluorescence correction).

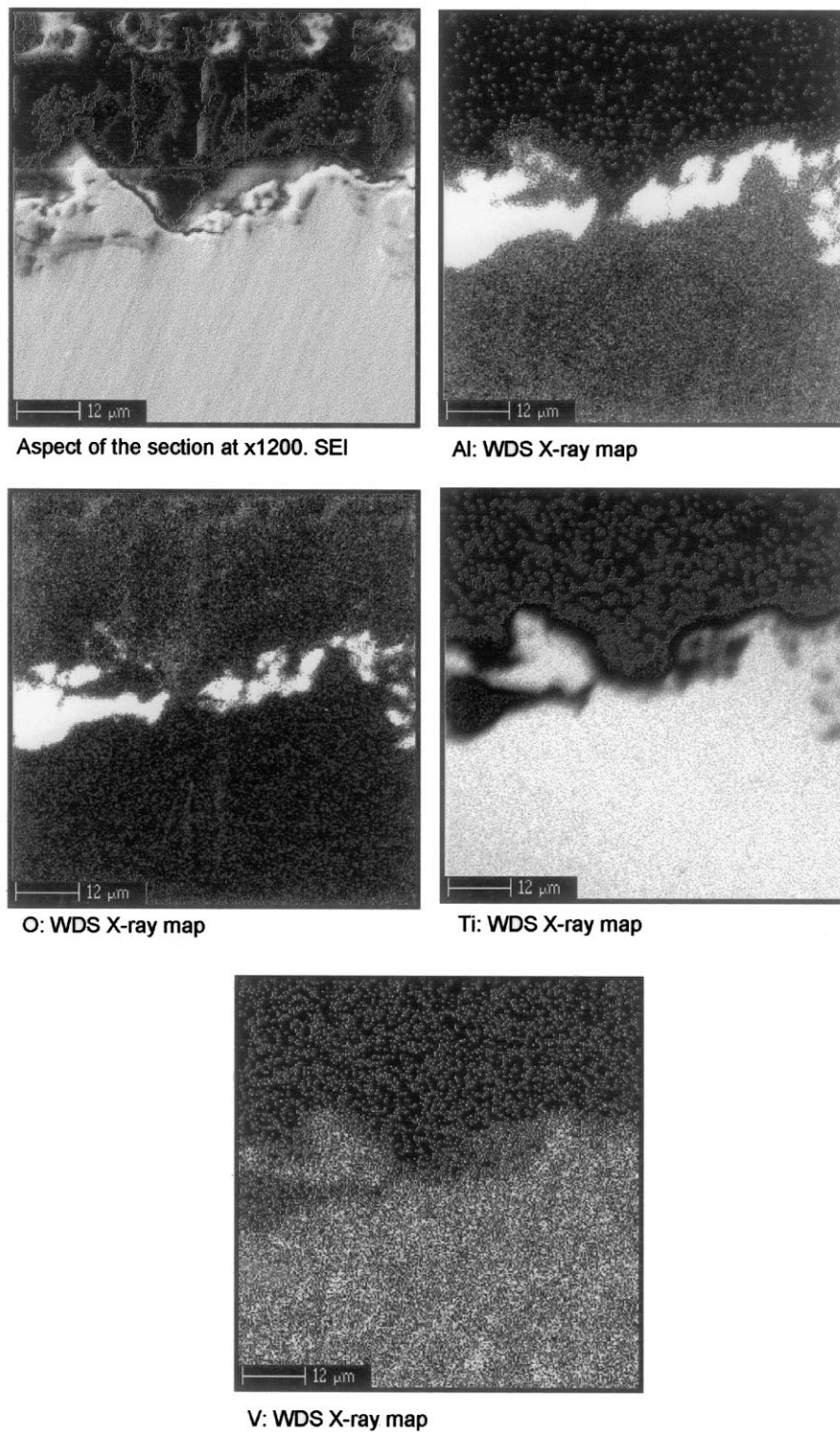


Fig. 3. WDS section analysis of the 500 μm alumina particles sand-blasted sample revealed an enrichment of surface with an oxidized aluminium compound (AlO_x) (white area), (magnification: $\times 1200$).

3. Results

3.1. Roughness measurement

Roughness parameters were calculated and are presented in Table 1. Roughness evaluated by R_a , R_t ,

Z_{max} , Z_{min} was higher on the sand-blasted than on the mirror-polished surfaces.

3.2. Chemical surface analysis

The WDS surface analysis of mechanically polished sample surfaces did not show any disturbance of the

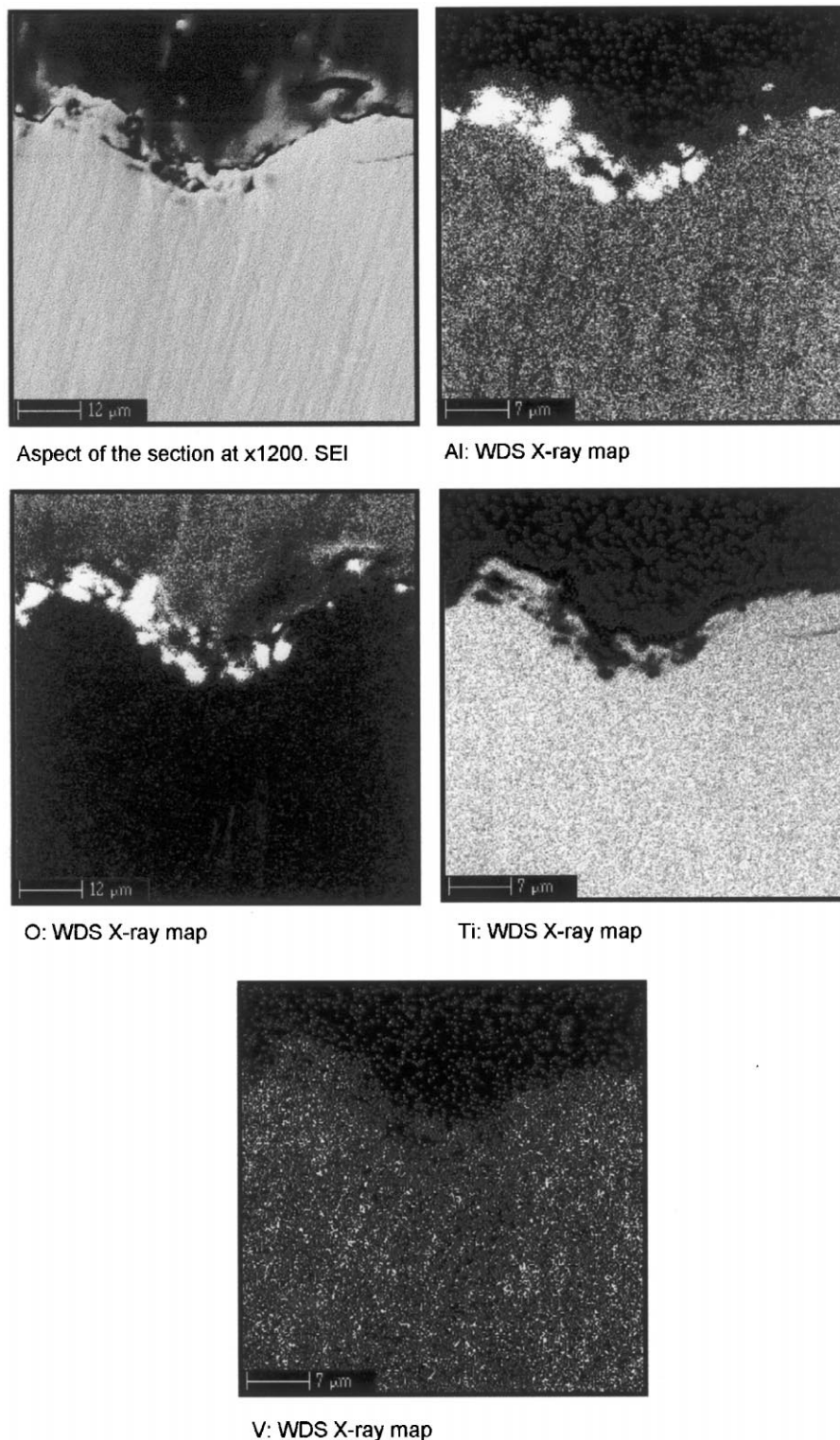


Fig. 4. WDS section analysis of the SiC sand-blasted sample. Same observations than on Fig. 3 (magnification: $\times 1200$).

topographical distribution of the main elements contained in the Ti6Al4V alloy, i.e. Al, Ti, V (Fig. 1).

On the other hand, WDS analysis of alumina sand-blasted surfaces revealed an enrichment of an oxidized

aluminium compound (AlO_x) (Fig. 2). Astonishingly, for several reasons (texture, shape, cathodoluminescence phenomena, etc.) this oxidized aluminium compound appeared not to be systematically made up of the

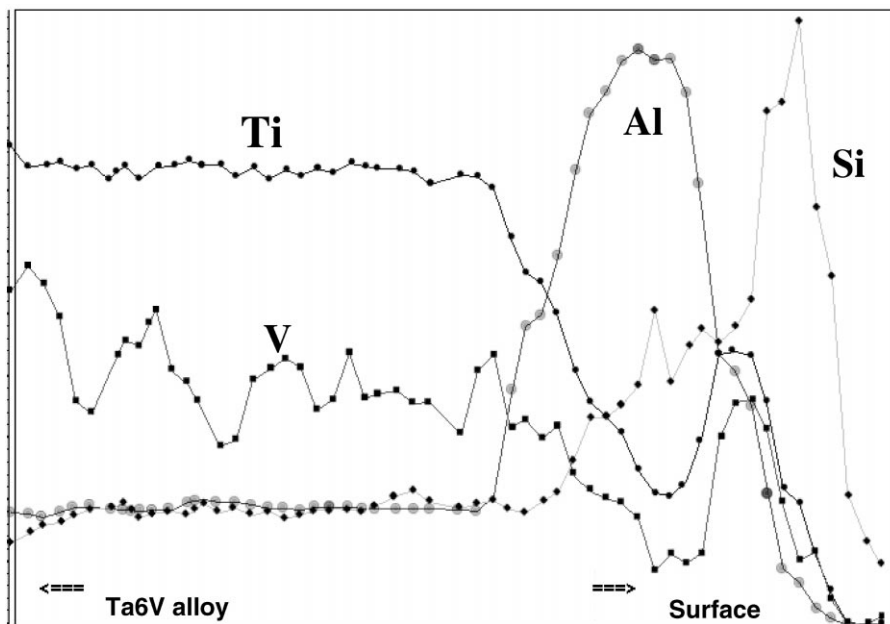


Fig. 5. WDS quantitative section analysis of the SiC sand-blasted alloy. Profiles of Ti, Al, Si and V weight concentrations revealed the Al enrichment but no V enrichment on the outermost surface of the sand-blasted alloy. Si enrichment of the surface was related to silicon carbide particles used for sand blasting.

single-phase Al_2O_3 . Section analysis (Fig. 3) confirmed this fact. Moreover, given the thickness of this oxidized layer detected on the surface of the samples, sometimes more than $10\ \mu\text{m}$, the formation of this layer undoubtedly originated from an important chemical transformation of the alloy (due to stresses generated by sand blasting) and not only from contamination by aluminium oxide originating from the alumina particles used for sand blasting. To confirm such an assertion, section analysis was carried out on control samples sand blasted with silicon carbide (SiC) particles. Once again, the X-ray dot maps (Fig. 4) revealed a great enrichment of aluminium in an oxidized form (AlO_x) on the surface of the sand-blasted alloy, in a layer several micrometers thick. Both of the quantitative section analyses performed on alumina or SiC sand-blasted samples revealed the Al enrichment but no V enrichment at the outermost surface of the alloy (Fig. 5).

3.3. Cell morphology

On sand-blasted surfaces, human osteoblasts never attained confluence, even after 14 days. They had a stellate shape with numerous filamentous extensions (Fig. 6a). On mechanically polished P1200 surfaces, after 14 days, a confluent cell layer covered the surfaces, masking the residual polishing grooves (Fig. 6c). After 1 day on P4000 surfaces, cells were still relatively sparse on the material surface but appeared very flattened (Fig. 6e).

On sand-blasted surfaces, after 3 days of culture, MC3T3-E1 cells had no particular orientation. They showed a round morphology with some filamentous extensions (Fig. 6b). On manually polished P80 surfaces, the cells were more spread, with dorsal ruffles demonstrating a high cellular activity (Fig. 6d). On P1200, P4000 and mirror-polished surfaces, cells were widely dispersed, with lamellipods demonstrating cell migration. On P1200 surfaces, cell orientation still followed residual grooves although on P4000 and mirror-polished surfaces no particular orientation of cells was observed (Fig. 6f).

3.4. Cell proliferation

The proliferation rate of MC3T3-E1 is related to the surface roughness. Proliferation decreased when surface roughness increased (Fig. 7a). In a similar manner, the proliferation index of human osteoblasts decreased when the surface roughness increased (Fig. 7b).

The analysis of variance of the proliferation rate showed that roughness was a significant influencing factor on MC3T3-E1 proliferation ($P < 0.03$) and on human osteoblast proliferation ($P < 0.02$). Moreover, a high correlation existed between the roughness R_a parameter and the proliferation rate of MC3T3-E1 cells ($r^2 = 0.922$) or the proliferation index of human osteoblasts ($r^2 = 0.914$).

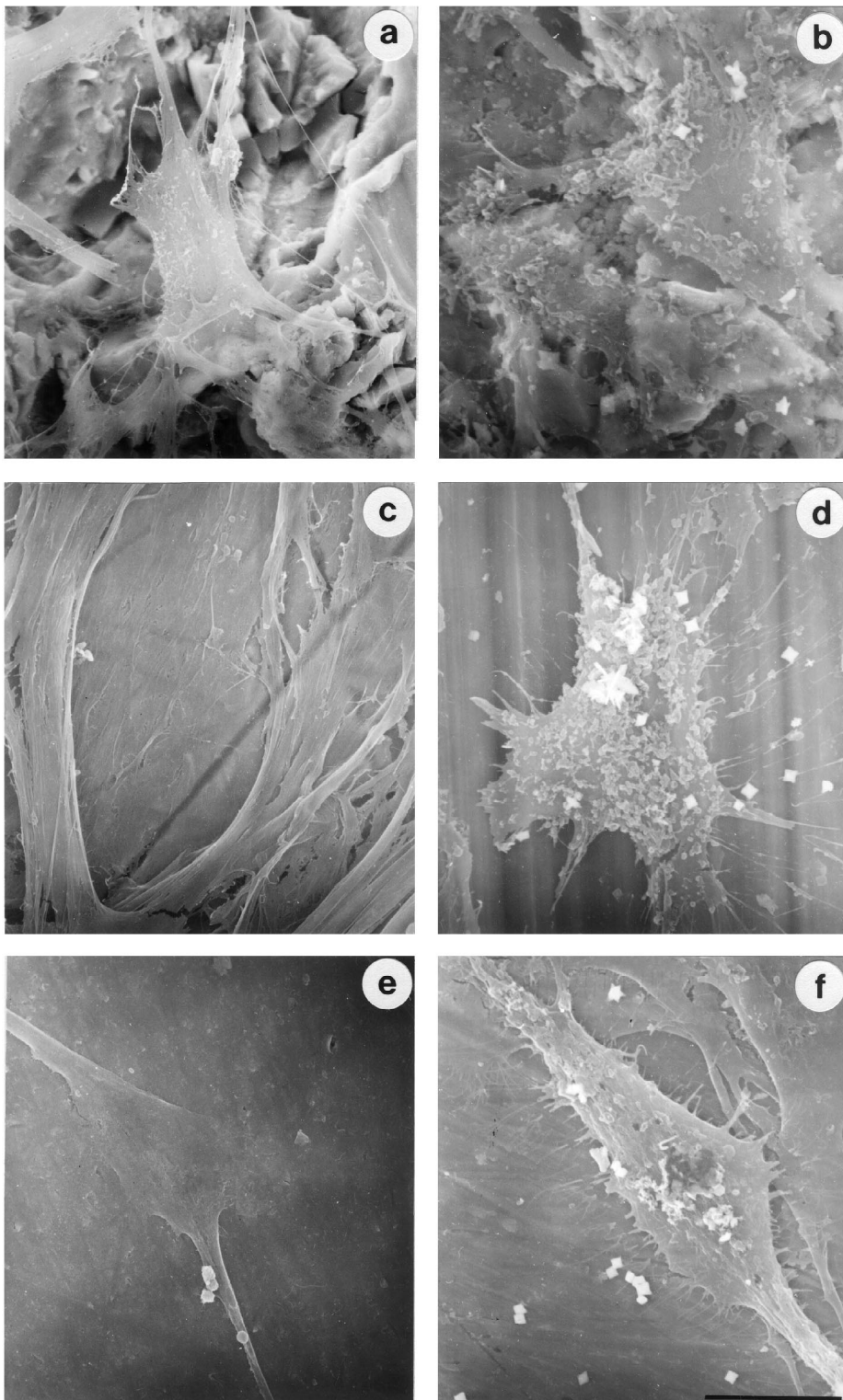


Fig. 6. SEM micrographs of osteoblastic cells on tested samples: (a) human osteoblasts after 14 days on S500 μm , (b) MC3T3-E1 osteoblastic cells after 3 days on S500 μm , (c) human osteoblasts after 14 days on P1200, (d) MC3T3-E1 osteoblastic cells after 3 days on P80, (e) human osteoblasts after 1 day on P4000, (f) MC3T3-E1 osteoblastic cells after 3 days on mirror-polished.

3.5. Cell adhesion

The human osteoblast detachment index decreased, i.e. adhesion increased, on all surfaces as a function of time

(Fig. 8). For 3 mm sand-blasted samples, there was no difference in adhesion whatever the culture time span. Therefore, adhesion on 3 mm sand-blasted samples remained weak at each delay from 1 to 21 days.

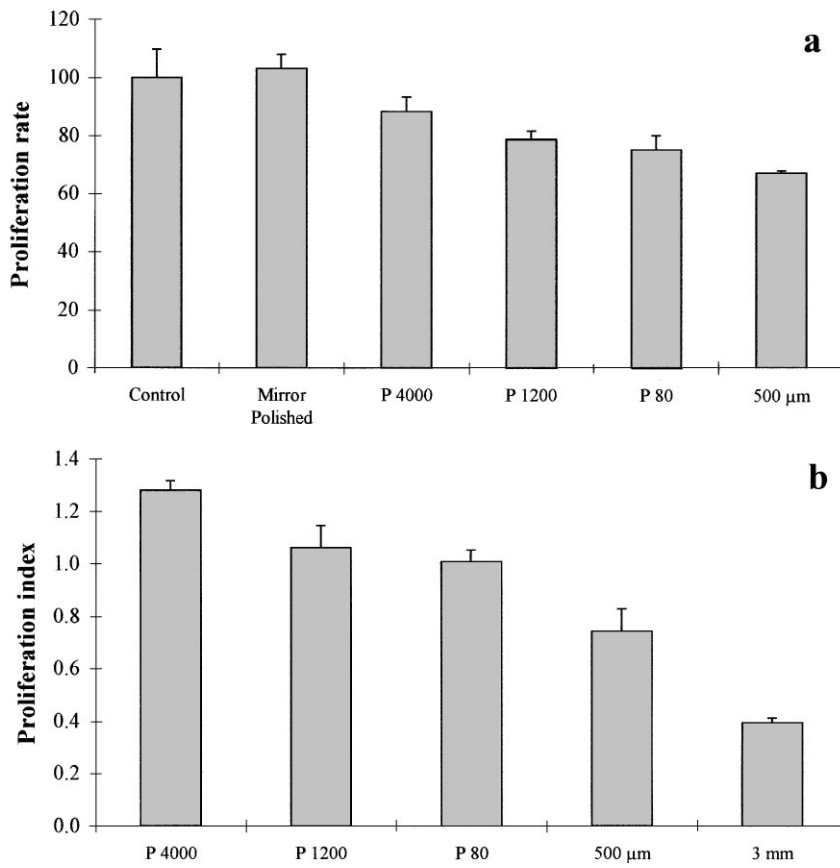


Fig. 7. (a) MC3T3-E1 osteoblastic cells proliferation rate after 3 days in culture on Ti6Al4V samples with varied surface roughnesses. (b) Proliferation index of human osteoblasts cultured on Ti6Al4V samples with varied surface roughnesses.

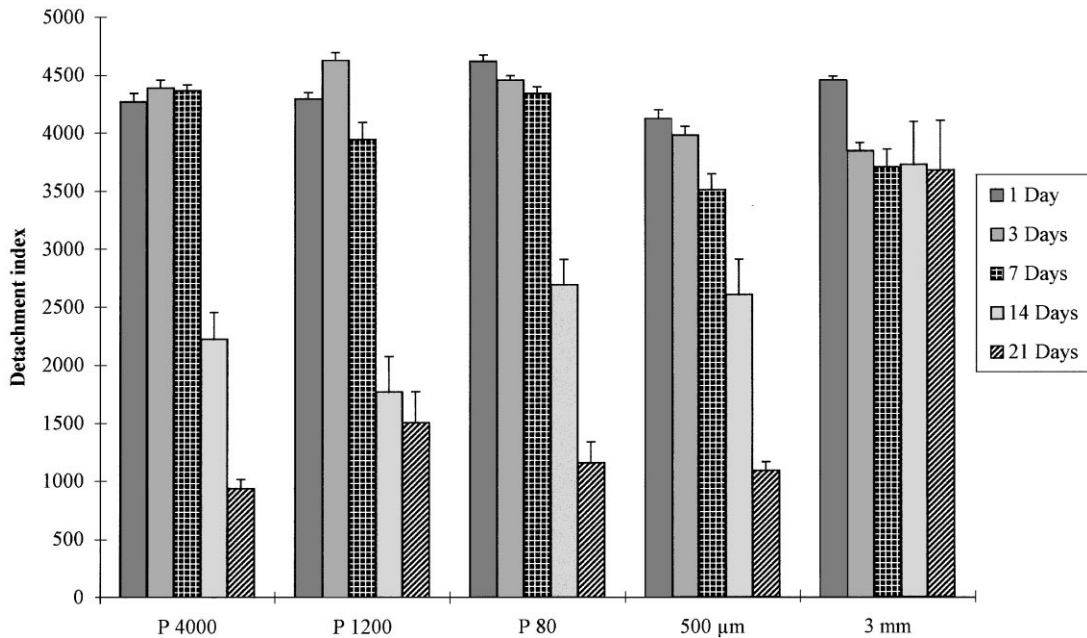


Fig. 8. Detachment index histogram on the various tested surfaces as a function of time.

4. Discussion

We compared the behaviour of a mouse osteoblastic cell line (MC3T3-E1) and of primary human osteoblastic cells on the Ti6Al4V samples with various surface roughnesses. Morphologically, the two cell lines reacted homogeneously in respect to surface roughness: cells were more spread on smooth surfaces than on rough ones. Contrary to previous reports on in vitro tests [24–26] or in vivo tests [6,8], we observed a lower proliferation and adhesion on rough surfaces than on smooth ones. However, our results are in accordance with many other in vitro tests concerning the proliferation of osteoblastic cells [19–21,27,28], fibroblastic cells [17] or epithelial cells [29].

The organization of surface roughness is an important parameter to consider. As previously described, we also observed that MC3T3-E1 cells generally followed residual groove orientation [30,31]. On the other hand, human osteoblasts ‘ignored’ the underlying residual grooves and covered the surface with a confluent layer. The difference in the organization of residual grooves may explain these varied reactions in the two tested cell lines. We have previously demonstrated the influence of roughness organization as evaluated by fractal analysis on human bone cell adhesion [18]. The role of surface roughness regularity on osteoblast-like MG63 cells differentiation and calcification has also been discussed by Martin et al. [21].

Additionally, Larsson et al. underlined the influence of surface topography and oxide thickness in the bone response to titanium implants [9]. Surfaces are different from the corresponding bulk of the material, and contain reactive bonds which in turn lead to the formation of a surface reactive layer (e.g. surface oxides on metals) and adsorbed contamination layers [32]. As previously described, surface preparation techniques such as cleaning, sterilization or machining-induced chemical surface disturbances [1,7,18–21,33–37]. By WDS surface analysis, we demonstrated that sand-blasting treatment totally disturbed the Ti6Al4V alloys’ chemical surface composition. We observed surface enrichment by AlO_x elements. The machining of Ti6Al4V alloys has previously been shown to induce the formation of a concentration of aluminium oxides on the outermost surface [22]. These authors call special attention to these concentrations of Al on the machined implant surfaces since they constitute a potential risk of Al dissolution in the biological fluids surrounding alloyed Ti surgical implants [22]. In our case, the Al dissolution from the surface may also explain our lower proliferation rate on sand-blasted surfaces. In further experiments, the Al contents in the underlying culture medium or in adherent cells should be monitored. Consequently, the differences we report in this experiment cannot be clearly related neither to Ti6Al4V substrates roughness nor to surface chemistry alter-

ations. Further experiments are under investigation to dissociate more clearly surface topography and surface chemistry effects on human osteoblast adhesion.

Additionally, our results highlight the necessity of taking into consideration not only roughness aspects but also the physico-chemical composition of biomaterial surfaces for the interpretation of in vitro cytocompatibility and in vivo biocompatibility results. In particular, we demonstrated that an usual surface preparation for increasing the bone integration of Ti6Al4V surgical implants (i.e. sand blasting) may extensively transform their chemical surface composition. Therefore, the expected bone integration of implants may be extensively impaired by surface treatments.

This phenomenon, widely known in the field of metallurgy, is not sufficiently taken into account in the field of biomaterials. We call special attention in this paper to the crucial significance of chemical surface analysis after any surface preparation treatment of metallic implants and especially titanium-based ones before any biological use.

Acknowledgements

The authors wish to thank SH industries (Marly, France) for kindly supplying the Ti6Al4V metal bars, B. Noël for cell culture preparation, E. Dufresne for surface processing, and D. Judas (CRITT Céramiques Fines, Maubeuge, France) for sand-blasting processing. This work was supported by the Fédération Biomatériaux Nord/Pas-de-Calais.

References

- [1] Swart KM, Keller JC, Wightman JP, Draughn RA, Stanford CM, Michaels CM. Short-term plasma-cleaning treatments enhance in vitro osteoblast attachment to titanium. *J Oral Implantol* 1992;18:130–7.
- [2] Bordji K, Jouzeau JY, Mainard D, Payan E, Netter P, Rie KT, Stucky T, Hage-Ali M. Cytocompatibility of Ti-6Al-4V and Ti-5Al-2.5Fe alloys according to three surface treatments, using human fibroblasts and osteoblasts. *Biomaterials* 1996; 17:929–40.
- [3] Vrouwenvelder WCA, Groot CG, de Groot K. Histological and biochemical evaluation of osteoblasts cultured on bioactive glass, hydroxyapatite, titanium alloy and stainless steel. *J Biomed Mater Res* 1993;27:465–75.
- [4] Itakura Y, Kosugi A, Sudo H, Yamamoto S, Kumegawa M. Development of a new system for evaluating the biocompatibility of implant materials using an osteogenic cell line (MC3T3-E1). *J Biomed Mater Res* 1988;22:613–22.
- [5] Klokkevold PR, Nishimura RD, Adachi M, Caputo A. Osseointegration enhanced by chemical etching of the titanium surface. *Clin Oral Implant Res* 1997;8:442–7.
- [6] Buser D, Schenk RK, Steinemann S, Fiorellini JP, Fox CH, Stich H. Influence of surface characteristics on bone integration of titanium implants. A histomorphometric study in miniature pigs. *J Biomed Mater Res* 1991;25:889–902.

- [7] Hazan R, Brener R, Oron U. Bone growth to metal implants is regulated by their chemical properties. *Biomaterials* 1993; 14:570–4.
- [8] Thomas KA, Cook SD. An evaluation of variables influencing implant fixation by direct bone apposition. *J Biomed Mater Res* 1985;19:875–901.
- [9] Larsson G, Thomsen P, Aronsson BO, Rodhal M, Lausmaa J, Kasemo B, Ericson LE. Bone response to surface-modified titanium implants: studies on the early tissue response to machined and electropolished implants with different oxide thicknesses. *Biomaterials* 1996;17:605–16.
- [10] Wennerberg A, Ektessabi A, Albrektsson T, Johansson C, Andersson B. A 1-year follow-up of implants of different surface roughness placed in rabbit bone. *Int J Oral Maxillofac Implants* 1997; 12:486–94.
- [11] Maurer AM, Merritt K, Brown SA. Cellular uptake of titanium and vanadium from addition of salts or fretting corrosion in vitro. *J Biomed Mater Res* 1994;28:241–6.
- [12] Wang JY, Wicklund BH, Gustilo RB, Tsukayama DT. Prosthetic metals interfere with the functions of human osteoblast cells in vitro. *Clin Orthop Relat Res* 1997;339:216–26.
- [13] Rae T. The biological response to titanium and titanium–aluminum–vanadium alloy particles. *Biomaterials* 1986;7:30–40.
- [14] Evans EJ. Cell damage in vitro following direct contact with fine particules of titanium, titanium alloy and cobalt-chrome-molybdenum alloy. *Biomaterials* 1994;15:713–7.
- [15] Squire MW, Ricci JL, Bizios R. Analysis of osteoblast mineral deposits on orthopaedic/dental implant metals. *Biomaterials* 1996;17:725–33.
- [16] Yao J, Glant TT, Lark MW, Mikecz K, Jacobs JJ, Hutchinson NI, Hoerrner LA, Kuettner KE, Galante JO. The potential role of fibroblasts in periprosthetic osteolysis: fibroblast response to titanium particles. *J Bone Miner Res* 1995;10:1417–27.
- [17] Könönen M, Hormia M, Kivilahti J, Hautaniemi J, Thesleff I. Effect of surface processing on the attachment orientation, and proliferation of human gingival fibroblasts on titanium. *J Biomed Mater Res* 1992;26:1325–41.
- [18] Anselme K, Bigerelle M, Noel B, Dufresne E, Judas D, Iost A, Hardouin P. Qualitative and quantitative study of human osteoblast adhesion on materials with various surface roughness. *J Biomed Mater Res* 2000;49:155–66.
- [19] Kieswetter K, Schwartz Z, Hummert TW, Cochran DL, Simpson J, Dean DD, et al. Surface roughness modulates the local production of growth factors and cytokines by osteoblast-like MG-63 cells. *J Biomed Mater Res* 1996;32:55–63.
- [20] Boyan BD, Batzer R, Kieswetter K, Liu Y, Cochran DL, Szmuckler-Moncler S, et al. Titanium surface roughness alters responsiveness of MG63 osteoblast-like cells to $1\alpha,25\text{-(OH)}_2\text{D}_3$. *J Biomed Mater Res* 1998;39:77–85.
- [21] Martin JY, Schwartz Z, Hummert TW, Schraub DM, Simpson J, Lankford J, et al. Effect of titanium surface roughness on proliferation, differentiation, and protein synthesis of human osteoblast-like cells (MG63). *J Biomed Mater Res* 1995; 29:389–401.
- [22] Ask M, Lausmaa J, Kasemo B. Preparation and surface spectroscopic characterization of oxide films on Ti6Al4V. *Appl Surf Sci* 1988;35:283–301.
- [23] Anselme K, Lanel B, Gentil C, Hardouin P, Marie PJ, Sigot-Luizard MF. Bone organotypic culture method: a model for cytocompatibility testing of biomaterials. *Cells Mater* 1994; 4:113–23.
- [24] Nishimura N, Kawai T. Effect of microstructure of titanium surface on the behaviour of osteogenic cell line MC3T3-E1. *J Mater Sci: Mater Med* 1998;9:99–102.
- [25] Keller JC, Stanford CM, Wightman JP, Draughn RA, Zaharias R. Characterizations of titanium implant surfaces, III. *J Biomed Mater Res* 1994;28:939–46.
- [26] Bowers KT, Keller JC, Randolph BA, Wick DG, Michaels CM. Optimization of surface micromorphology for enhanced osteoblast responses in vitro. *Int J Oral Maxillofac Implants* 1992; 7:302–10.
- [27] Naji A, Harmand MF. Study of the effect of the surface state on the cytocompatibility of a Co–Cr alloy using human osteoblasts and fibroblasts. *J Biomed Mater Res* 1990;24:861–71.
- [28] De Santis D, Guerriero C, Nocini PF, Ungersbock A, Richards G, Gotte P, et al. Adult human bone cells from jaw bones cultured on plasma-sprayed or polished surfaces of titanium or hydroxyapatite discs. *J Mater Sci: Mater Med* 1996;7:21–8.
- [29] Chehroudi B, Gould TRL, Brunette DM. Effects of a grooved titanium-coated implant surface on epithelial cell behavior in vitro and in vivo. *J Biomed Mater Res* 1989;23:1067–85.
- [30] Chesmel KD, Clark CC, Brighton CT, Black J. Cellular responses to chemical and morphologic aspects of biomaterial surfaces. II. The biosynthetic and migratory response of bone cell populations. *J Biomed Mater Res* 1995;29:1101–10.
- [31] Brunette DM, Ratkay J, Chehroudi B. Behaviour of osteoblasts on micromachined surfaces. In: Davies JE, editor. *The bone–biomaterial interface*. Toronto: University of Toronto Press, 1991. p. 170–80.
- [32] Kasemo B, Lausmaa J. Material–tissue interfaces: the role of surface properties and processes. *Environ Health Perspect* 1994;102:41–5.
- [33] Kasemo B, Lausmaa J. Biomaterial and implant surfaces: on the role of cleanliness, contamination and preparation procedures. *J Biomed Mater Res* 1988;22:145–58.
- [34] Aronsson BO, Lausmaa J, Kasemo B. Glow discharge plasma treatment for surface cleaning and modification of metallic biomaterials. *J Biomed Mater Res* 1997;35:49–73.
- [35] Vezeau PJ, Koorbusch GF, Draughn RA, Keller JC. Effects of multiple sterilization on surface characteristics and in vitro biologic responses to titanium. *J Oral Maxillofac Surg* 1996;54:738–46.
- [36] Stanford CM, Keller JC, Solursh M. Bone cell expression on titanium surfaces is altered by sterilization treatments. *J Dent Res* 1994;73:1061–71.
- [37] Baier RE, Meyer AE, Akers CK, Natiella JR, Meenaghan M, Carter JM, Meenaghan MCJ. Degradative effects of conventional steam sterilization on biomaterial surfaces. *Biomaterials* 1982; 3:241–5.